Simulating Permian–Triassic oceanic anoxia distribution: Implications for species extinction and recovery

Cornelia Winguth and Arne M.E. Winguth
Department of Earth and Environmental Sciences, University of Texas at Arlington, Arlington, Texas 76019, USA

ABSTRACT

The biggest mass extinction in the Phanerozoic, at the end of the Permian, has been associated with oceanic changes, but the exact dynamics are still debated. Intensified stratification, widespread anoxia, chemocline excursions, and large-scale ocean overturn events have all been invoked as contributors to the extinction. In this study the effects of possible changes in environmental conditions, such as an increase in nutrient input or dust fluxes into the ocean or an intensification of the biological pump, on Permian–Triassic ocean chemistry are investigated. Series of sensitivity experiments were performed with a fully coupled climate-carbon cycle model. None of the forcings alone generates extensive low-oxygen conditions in the deep sea. These are only simulated by an intense eutrophication in combination with an enhanced biological pump, but still confined to the central Panthalassic, Tethys, and the eastern Boreal Oceans. Our findings support the conclusions from a recent geochemical study of a Japanese deep Panthalassa section, that around the Permian-Triassic boundary, the oxygen minimum zone expanded considerably, while the deep Panthalassa remained ventilated. The warming-induced increase in low-oxygen conditions within the water column aggravated adverse existing conditions and likely contributed to the extinction peak. Upwelling of toxic water was probably regionally confined and hence not the main cause for the end-Permian marine and terrestrial mass extinction. Widespread deep-sea anoxia, generated by a strong increase in weathering and the related enhanced nutrient input into the oceans, is probably closely linked to the delayed recovery of species in the Early Triassic.

INTRODUCTION

The Permian-Triassic boundary (PTB, ca. 252 Ma; Mundil et al., 2010) is characterized by the most severe Phanerozoic mass extinction, with disappearance of an estimated ~90% of all marine species and widespread devastation of terrestrial ecosystems (Erwin, 1994). The recovery of species in the Early Triassic happened slowly (e.g., Payne et al., 2004). Many hypotheses about the causes and dynamics of the PTB mass extinction and the delayed recovery have been linked to intensified ocean stratification and anoxic oceanic environments in the context of large environmental changes, triggered by the eruption of the Siberian flood basalts (e.g., Campbell et al., 1992; Wignall and Twitchett, 1996; Berner, 2005). The extent of ocean anoxia, however, remains controversial, especially for the deep sea. A brief euxinic episode at the end of the Permian, embedded in a prolonged interval of Panthalassic anoxia, was described by Isozaki (1997) for two deep-sea sections. Algeo et al. (2010) postulated, based on accreted deep-sea material in a Japanese section, that the expansion of low-oxygen conditions in the Panthalassa was concentrated in the intermediate-water oxygen minimum zone (OMZ).

Other subjects of debate are the causes of the anoxic or euxinic conditions. Several model studies have suggested that the ocean circulation was more sluggish than today, but that ocean stagnation, which had been invoked as a main explanation for benthic anoxic conditions, is unlikely (e.g., Zhang et al., 2001; Winguth and Maier-Reimer, 2005). Volcanism-induced warming may have led to a drastic increase in soil and subsequent bedrock weathering and hence nutrient delivery to the ocean, high productivity, and eventually anoxic conditions (Sephton et al., 2005; Meyer et al., 2008; Algeo et al., 2010). The spreading of anoxic conditions, the overturn of an anoxic ocean, and/or sulfide escaping into the atmosphere, leading to a loss of ozone and hence dramatic radiative impacts on land, have been discussed as causes for the mass extinction (e.g., Knoll et al., 1996; Wignall and Twitchett, 1996; Kump et al., 2005).

Herein the PTB event is investigated through several sensitivity experiments with a fully coupled climate and carbon cycle model. The results are used to constrain the impact of changes in nutrient input and the sinking flux of organic material on the marine environment. By assessing the expansion of low-oxygen or anoxic conditions with increases in nutrient availability, also in combination with an enhanced particle transport to the deep sea, their possible role in the causation or prolongation of adverse conditions for organisms at that time is evaluated.

EXPERIMENT SETUP

The fully-coupled Community Climate System Model (version 3, CCSM3; Collins et al., 2006), consisting of atmosphere, ocean, land, and sea-ice components, is used for end-Permian climate simulations. The atmosphere model resolution is T31 (3.75° × 3.75°) and 26 layers, while the ocean is modeled with a nominal resolution of 3° and 25 layers. This work represents a continuation of the study done by Kiehl and Shields (2005), who showed that with a constant atmospheric CO_2 concentration of 3550 ppmv (~12.7× the preindustrial level), modeled land and ocean temperatures are in general agreement with paleodata. The weak simulated overturning circulation of ~10 Sv at depth, together with the high modeled ideal ages, led Kiehl and Shields (2005) to the conclusion that suppressed oxygen and nutrient delivery to the deep ocean resulted in widespread anoxia. In order to test this hypothesis as well as to investigate the effects of various potential forcings on Permian–Triassic ocean chemistry, we have added a carbon cycle model (described in Doney et al., 2006) to the existing 2700 yr simulation. The biological uptake of PO_4 is determined by the turnover of biomass, modulated by surface solar irradiance, temperature, macronutrients, and micronutrients. The vertical particulate organic carbon flux is described by a Martin power-law curve, in which the exponent determines the degree of flux attenuation with depth. More model details are given in the GSA Data Repository[1].

The model was integrated for 2500 additional years for the PTB reference experiment (using boundary conditions from Kiehl and Shields, 2005) and for several sensitivity experiments. The impacts of intensification in weathering were tested by oceanic phosphate inventory increases to 2×, 4×, and 10× the modern value. A simulation with 10× the Fe supply of the reference experiment was carried out to investigate the influence of dust ejected into the atmosphere by intense volcanism on marine environments. A change to a less effective food web at the PTB (Broecker and Peacock, 1999) as well as an increase in primary productivity due to ocean fertilization might have intensified the transport of organic carbon to abyssal layers. In order to simulate an enhanced pump, we changed the exponent in the Martin parameterization from 0.9 to 0.5, consistent with deeper particle penetration in a higher productivity zone identified by Buesseler et al. (2007). In one sensitivity

[1]GSA Data Repository item 2012037, biogeochemical model description, model comparison, and additional model results, is available online at www.geosociety.org/pubs/ft2012.htm, or on request from editing@geosociety.org or Documents Secretary, GSA, P.O. Box 9140, Boulder, CO 80301, USA.

experiment, the enhanced pump was combined with the 10× phosphate content.

The findings of these simulations are compared with those of an approximately three times lower resolution model study by Meyer et al. (2008), who used the GENIE-1 model forced with the CCSM3 boundary conditions of Kiehl and Shields (2005).

RESULTS

When keeping nutrient levels at modern values, the deep sea, with dissolved oxygen concentration, [O_2], values of >125 mmol L^{-1}, remains well oxygenated throughout the Panthalassic as well as the Tethys Oceans (Fig. 1). An OMZ is simulated in the eastern equatorial Panthalassa between 400 m and 800 m water depth (Fig. 2), but not in the Tethys Ocean. The OMZ is correlated with higher surface productivity in this area, induced by nutrient-rich coastal upwelling (Fig. 3).

With an increase of the oceanic phosphate content to 2×, 4×, and 10× the reference inventory, the export production of particulate organic carbon increases accordingly due to higher nutrient availability in the euphotic zone (Fig. 3). Overall, high productivity is modeled in the upwelling areas of eastern Panthalassa as well as in mid-latitude coastal regions of western Panthalassa. For the 10× PO_4 experiment, productivity also strongly increases in most of the Tethys Ocean, consistent with the concept that basins act as nutrient traps (e.g., Meyer et al., 2008).

Higher productivity generates higher oxygen demand for the decomposition and remineralization process in the water column as well as in the deep sea. The OMZ expands vertically and horizontally with increasing nutrient contents, until at 10× PO_4, it extends across all of the equatorial Panthalassic and Tethys Oceans, as well as the southern Boreal Ocean (Fig. DR1 in the Data Repository). The deep-sea zone of <20 mmol L^{-1} [O_2] is confined to the area beneath highest productivity in the easternmost Panthalassa in the 2× PO_4 experiment (Fig. 1). It expands considerably for the 4× PO_4 case, with lowest [O_2] of 0–5 mmol L^{-1} in the eastern Panthalassa and the southernmost Tethys Oceans, and in the 10× PO_4 scenario, the western half of the deep Tethys as well as an extensive part of the equatorial eastern Panthalassa are oxygen depleted (Fig. 1). Increased dust supply, parameterized by 10× Fe, results in an increase in export production and an accompanying mild decrease of oxygen levels mainly at high latitudes, but deep-ocean [O_2] values remain >120 mmol L^{-1} at all locations. The OMZ extends downward to ~1800 m when applying the enhanced biological pump parameterization to the reference run, while the deep-sea dissolved oxygen content remains >20 mmol L^{-1} except for a very small area in the equatorial eastern Panthalassa. Only an enhanced pump parameterization in combination with a significant eutrophication (10× PO_4) results in widespread anoxic conditions throughout the central deep Panthalassa and all of the deep Tethys Oceans, as well as the eastern Boreal Ocean (Fig. 1). Anoxia extends downward from ~80 m below sea level in a small area of the equatorial Panthalassa in the 10× PO_4 experiment, and from deeper levels for lower

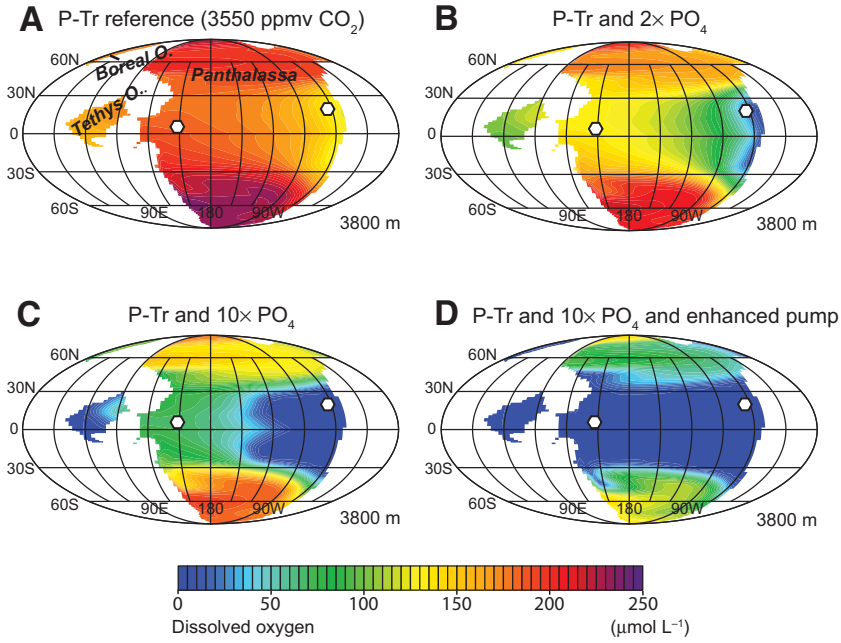

Figure 1. A: Dissolved oxygen (50 yr mean; in mmol L^{-1}) at ~3800 m depth for Permian-Triassic (P-Tr) boundary reference experiment. B: 2× PO_4 experiment. C: 10× PO_4 experiment. D: 10× PO_4 and enhanced pump experiment. White dots mark locations of Isozaki (1997) data in Panthalassa. Only an enhanced pump in combination with strong eutrophication generates widespread deep-sea anoxia.

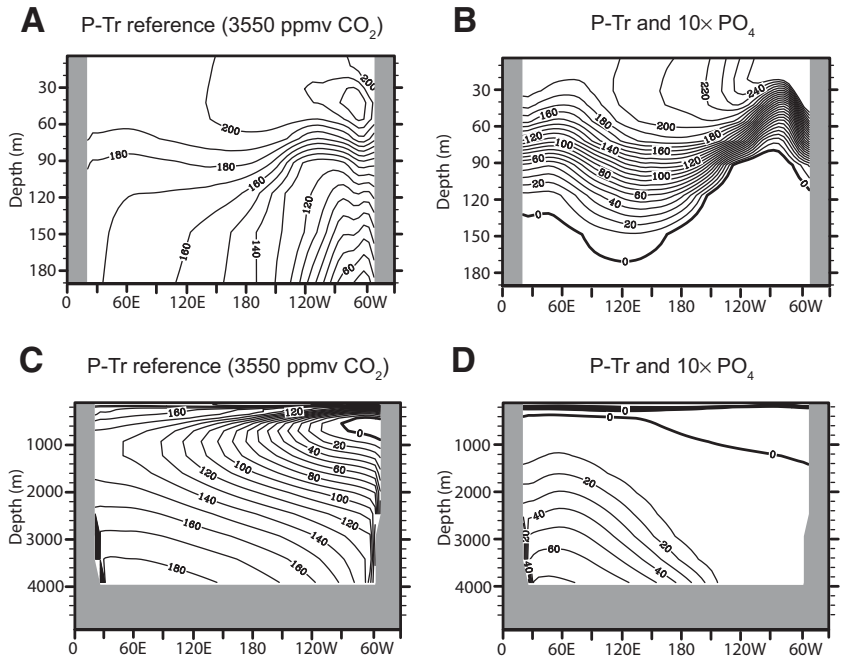

Figure 2. A: Equatorial Panthalassa cross section of dissolved oxygen (50 yr mean; in mmol L^{-1}) for Permian-Triassic (P-Tr) boundary reference run, upper 200 m. B: 10× PO_4 experiment, upper 200 m. C: PTB reference run, 4000 m. D: 10× PO_4 experiment, 4000 m. Oxygen minimum zone expands horizontally and vertically for increasing nutrient availability, but surface layer remains well oxygenated.

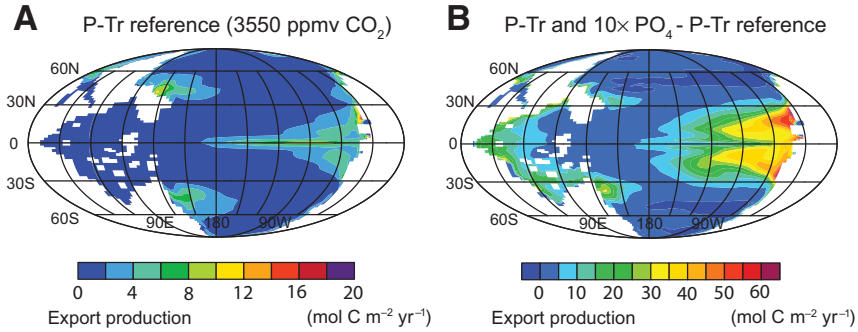

Figure 3. A: Particulate organic carbon export production (50 yr mean; in mol C m^{-2} yr^{-1}) for Permian-Triassic (P-Tr) boundary reference experiment. B: Shown as difference between 10× PO_4 experiment and reference experiment. For higher nutrient inventory, surface productivity increases in eastern equatorial Panthalassa due to upwelling and in Tethys Ocean due to nutrient trapping.

phosphate contents (Fig. 2). The ocean surface layer remains well mixed and oxygenated.

DISCUSSION

Comparison with Previous Model Results and Data

The OMZ results for the Panthalassic and Tethys Oceans are consistent with several simulations (see Winguth and Maier-Reimer, 2005), but in contrast to the low [O_2] of <1 mmol L^{-1} in the Tethys versus >150 mmol L^{-1} in Panthalassa described by Meyer et al. (2008). In agreement with Meyer et al. (2008) and other modeling studies (e.g., Zhang et al., 2001), our results indicate that the response of the ocean circulation to atmospheric CO_2-induced (3550 ppmv) warming alone cannot explain a widespread presence of anoxia. However, contrary to Meyer et al. (2008), even intense nutrient input (10× PO_4) leads to only regionally limited low-oxygen conditions. A combination of eutrophication with enhanced pumping is required to generate anoxia across the central Panthalassic, Tethys, and southern Boreal Oceans. Deep-water formation, although reduced relative to modern conditions, ventilates the mid- to high-latitude deep Panthalassa. The discrepancies in model results arise from the differences in resolution and in complexity of the parameterizations of convection, mixing, and diffusion (for a more detailed model comparison, see the Data Repository).

Although the atmospheric CO_2 concentration used in this study is at the higher end of the estimated range for the end-Permian (Breecker et al., 2010), the modeled meridional sea surface temperature gradient is still ~5 °C higher than the low-gradient scenario investigated by Hotinski et al. (2001), which yielded significant ocean stratification, weak deep-sea ventilation, and widespread anoxia at the seafloor. An effect that might have lowered the temperature gradient and hence enhanced anoxia is albedo reduction due to a decrease in the availability of cloud condensation nuclei in a low-productivity, high-temperature world (Kump and Pollard, 2008). Subsequent eutrophication and productivity increase, however, would have led to an abundant supply of cloud condensation nuclei, an increase in albedo, and an overall cooling effect.

A sulfidic water column has been suggested from pyrite findings and euxinia in the photic zone from biomarkers for parts of the southern Tethys (e.g., Grice et al., 2005), the northern Tethys (e.g., Cao et al., 2009), and the Boreal Ocean (Nielsen and Shen, 2004). Anoxic conditions in the lowermost photic zone are modeled at a few locations in these basins with 4× PO_4, and more extensively with 10× PO_4. Simulated upper layer [O_2] values in the Tethys region are highest in the south, in agreement with local oxic photic zone conditions inferred by Wignall and Twitchett (2002). Environmental conditions are much less well documented for the large Panthalassic Ocean (Algeo et al., 2010). Our model results for the 4× and 10× PO_4 experiments can be reconciled with deep-sea near-anoxic conditions at the British Columbia location in the eastern Panthalassa, described by Isozaki (1997), but not with the western Panthalassa section presented therein. Only in the most extreme 10× PO_4 and enhanced pump scenario, the simulated [O_2] value at this location is close to anoxic (Fig. 1). Algeo et al. (2010), however, attributed the lithologic changes in this area to an ~4–5× reduction in the sinking flux of biogenic silica and only a small shift toward more reducing bottom waters at the PTB. Algeo et al. (2010) inferred an expansion of the OMZ caused by changes in nutrient fluxes and/or primary productivity rates, while the areas below the OMZ could have served as refugia for certain species. Also, benthic oxygen-requiring epifaunal macroinvertebrates were present in the Tethys Ocean at the time of the PTB (Grice et al., 2005). This scenario correlates well with no change or a doubling of the nutrient input in our experiments.

Implications for the Permian–Triassic Mass Extinction and Recovery

While some increase in weathering has been inferred from soil-derived biomarkers for times preceding the end-Permian mass extinction event, more extensive bedrock erosion and hence nutrient delivery into the ocean took place during the Early Triassic (Sephton et al., 2005; Fenton et al., 2007; Cao et al., 2009; Algeo et al., 2011). Algeo and Twitchett (2010) calculated an ~7× mean global increase in the flux of eroded material to continent margins and platforms for the Early Triassic. Cyanobacteria thrived in the Early Triassic, probably from eutrophication (e.g., Chen et al., 2010) as well as from a decrease in grazing pressure after the PTB extinction event, which was characterized by a transient suppression of autotroph productivity (Algeo et al., 2011). The highest concentrations of biomarkers indicating photic-zone euxinia in the Tethys are reported for the Early Triassic (Grice et al., 2005), and the delayed Early Triassic recovery of species has been explained by high productivity in combination with a vigorous biological pump (Meyer et al., 2011). Based on these observations, it seems plausible that the experiments with little increase in the phosphate inventory correspond to the end-Permian situation, whereas higher nutrient inputs better represent the Early Triassic conditions. A progressively stronger impact of weathering on oxygen dissolution in the ocean, with anoxia starting to appear in the eastern Panthalassa for a doubling of PO_4, and spreading in the Tethys region for higher nutrient levels, can be reconciled with a diachronous extinction spreading from the western margin of Pangea to the Tethys region (Wignall and Newton, 2003). While intense bedrock weathering would have lowered atmospheric CO_2, prolonged volcanism and associated CO_2 and CH_4 release likely counteracted this effect.

CONCLUSIONS

Because strong weathering as a result of terrestrial ecosystem destruction did not fertilize the oceans until the Early Triassic, end-Permian conditions are better represented by the experiments with no or little nutrient increase. Anoxic conditions were confined to an expanded OMZ and the deep easternmost Panthalassa. Hence, upwelling of toxic euxinic waters might have occurred locally, adding to adverse conditions that had gradually developed throughout the Late Permian, but was probably not widespread across the globe and therefore not the main cause for the end-Permian terrestrial and marine mass extinctions. Nutrient-induced extensive anoxia was likely prevalent during the Early Triassic in the aftermath of the main extinction event, acting as a main factor in delaying species recovery.

ACKNOWLEDGMENTS

We thank Jeff Kiehl and Christine Shields for making available the Community Climate System Model version 3 Permian model files. The dust field for the 10× Fe simulation was provided by Natalie Mahowald. All model simulations were done on National Center for Atmospheric Research computers, supported by the National Science Foundation (NSF). The work is funded by NSF grant EAR-0745817. We thank two anonymous reviewers for their helpful comments on the manuscript.

REFERENCES CITED

Algeo, T.J., and Twitchett, R.J., 2010, Anomalous Early Triassic sediment fluxes due to elevated weathering rates and their biological consequences: Geology, v. 38, p. 1023–1026, doi:10.1130/G31203.1.

Algeo, T.J., Hinnov, L., Moser, J., Maynard, J.B., Elswick, E., Kuwahara, K., and Sano, H., 2010, Changes in productivity and redox conditions in the Panthalassic Ocean during the latest Permian: Geology, v. 38, p. 187–190, doi:10.1130/G30483.1.

Algeo, T.J., Chen, Z.Q., Fraiser, M.L., and Twitchett, R.J., 2011, Terrestrial-marine teleconnections in the collapse and rebuilding of Early Triassic marine ecosystems: Palaeogeography, Palaeoclimatology, Palaeoecology, v. 308, p. 1–11, doi:10.1016/j.palaeo.2011.01.011.

Berner, R.A., 2005, The carbon and sulfur cycles and atmospheric oxygen from middle Permian to Middle Triassic: Geochimica et Cosmochimica Acta, v. 69, p. 3211–3217, doi:10.1016/j.gca.2005.03.021.

Breecker, D.O., Sharp, Z.D., and McFadden, L.D., 2010, Atmospheric CO_2 concentrations during ancient greenhouse climates were similar to those predicted for A.D. 2100: National Academy of Sciences Proceedings, v. 107, p. 576–580, doi:10.1073/pnas.0902323106.

Broecker, W.S., and Peacock, S., 1999, An ecologic explanation for the Permo-Triassic carbon and sulfur isotope shifts: Global Biogeochemical Cycles, v. 13, p. 1167–1172, doi:10.1029/1999GB900066.

Buesseler, K.O., and 17 others, 2007, Revisiting carbon flux through the ocean's twilight zone: Science, v. 316, p. 567–570, doi:10.1126/science.1137959.

Campbell, I.H., Czamanske, G.K., Fedorenko, V.A., Hill, R.I., and Stepanov, V., 1992, Synchronism of the Siberian Traps and the Permian-Triassic boundary: Science, v. 258, p. 1760–1763, doi:10.1126/science.258.5089.1760.

Cao, C., Love, G.D., Hays, L.E., Wang, W., Shen, S., and Summons, R.E., 2009, Biogeochemical evidence for euxinic oceans and ecological disturbance presaging the end-Permian mass extinction event: Earth and Planetary Science Letters, v. 281, p. 188–201, doi:10.1016/j.epsl.2009.02.012.

Chen, L., Wang, Y., Xie, S., Kershaw, S., Dong, M., Yang, H., Liu, H., and Algeo, T.J., 2010, Molecular records of microbialites following the end-Permian mass extinction in Chongyang, Hubei Province, South China: Palaeogeography, Palaeoclimatology, Palaeoecology, v. 308, p. 151–159, doi:10.1016/j.palaeo.2010.09.010.

Collins, W.D., and 14 others, 2006, The Community Climate System Model Version 3 (CCSM3): Journal of Climate, v. 19, p. 2122–2143, doi:10.1175/JCLI3761.1.

Doney, S.C., Lindsay, K., Fung, I., and John, J., 2006, Natural variability in a stable 1000 year coupled climate-carbon cycle simulation: Journal of Climate, v. 19, p. 3033–3054, doi:10.1175/JCLI3783.1.

Erwin, D.H., 1994, The Permo-Triassic extinction: Nature, v. 367, p. 231–236, doi:10.1038/367231a0.

Fenton, S., Grice, K., Twitchett, R.J., Böttcher, M.E., Looy, C.V., and Nabbefeld, B., 2007, Changes in biomarker abundances and sulfur isotopes of pyrite across the Permian-Triassic (P/Tr) Schuchert Dal section (East Greenland): Earth and Planetary Science Letters, v. 262, p. 230–239, doi:10.1016/j.epsl.2007.07.033.

Grice, K., Cao, C., Love, G.D., Böttcher, M.E., Twitchett, R.J., Grosjean, E., Summons, R.E., Turgeon, S.C., Dunning, W., and Jin, Y., 2005, Photic zone euxinia during the Permian-Triassic superanoxic event: Science, v. 307, p. 706–709, doi:10.1126/science.1104323.

Hotinski, R.M., Bice, K.L., Kump, L.R., Najjar, R.G., and Arthur, M.A., 2001, Ocean stagnation and end-Permian anoxia: Geology, v. 29, p. 7–10, doi:10.1130/0091-7613(2001)029<0007:OSAEPA>2.0.CO;2.

Isozaki, Y., 1997, Permo-Triassic boundary superanoxia and stratified superocean; records from lost deep sea: Science, v. 276, p. 235–238, doi:10.1126/science.276.5310.235.

Kiehl, J.T., and Shields, C.A., 2005, Climate simulation of the latest Permian: Implications for mass extinction: Geology, v. 33, p. 757–760, doi:10.1130/G21654.1.

Knoll, A.H., Bambach, R.K., Canfield, D.E., and Grotzinger, J.P., 1996, Comparative Earth history and Late Permian mass extinction: Science, v. 273, p. 452–457, doi:10.1126/science.273.5274.452.

Kump, L.R., and Pollard, D., 2008, Amplification of Cretaceous warmth by biological cloud feedbacks: Science, v. 320, p. 195, doi:10.1126/science.1153883.

Kump, L.R., Pavlov, A., and Arthur, M.A., 2005, Massive release of hydrogen sulfide to the surface ocean and atmosphere during intervals of oceanic anoxia: Geology, v. 33, p. 397–400, doi:10.1130/G21295.1.

Meyer, K.M., Kump, L.R., and Ridgwell, A., 2008, Biogeochemical controls on photic-zone euxinia during the end-Permian mass extinction: Geology, v. 36, p. 747–750, doi:10.1130/G24618A.1.

Meyer, K.M., Yu, M., Jost, A.B., Kelley, B.M., and Payne, J.L., 2011, $\delta^{13}C$ evidence that high primary productivity delayed recovery from end-Permian mass extinction: Earth and Planetary Science Letters, v. 302, p. 378–384, doi:10.1016/j.epsl.2010.12.033.

Mundil, R., Pálfy, J., Renne, P.R., and Brack, P., 2010, The Triassic timescale: New constraints and a review of geochronological data, *in* Lucas, S.G., ed., The Triassic timescale: Geological Society of London Special Publication 334, p. 41–60, doi:10.1144/SP334.3.

Nielsen, J.K., and Shen, Y., 2004, Evidence for sulfidic deep water during the Late Permian in the East Greenland Basin: Geology, v. 32, p. 1037–1040, doi:10.1130/G20987.1.

Payne, J.L., Lehrmann, D.J., Wei, J., Orchard, M.J., Schrag, D.P., and Knoll, A.H., 2004, Large perturbations of the carbon cycle during recovery from the end-Permian extinction: Science, v. 305, p. 506–509, doi:10.1126/science.1097023.

Sephton, M.A., Looy, C.V., Brinkhuis, H., Wignall, P.B., de Leeuw, J.W., and Visscher, H., 2005, Catastrophic soil erosion during the end-Permian biotic crisis: Geology, v. 33, p. 941–944, doi:10.1130/G21784.1.

Wignall, P.B., and Newton, R., 2003, Contrasting deep-water records from the Upper Permian and Lower Triassic of South Tibet and British Columbia: Evidence for a diachronous mass extinction: Palaios, v. 18, p. 153–167, doi:10.1669/0883-1351(2003)18<153:CDRFTU>2.0.CO;2.

Wignall, P.B., and Twitchett, R.J., 1996, Oceanic anoxia and the end Permian mass extinction: Science, v. 272, p. 1155–1158, doi:10.1126/science.272.5265.1155.

Wignall, P.B., and Twitchett, R.J., 2002, Extent, duration and nature of the Permian-Triassic superanoxic event, *in* Koeberl, C., and MacLeod, K.C., eds., Catastrophic events and mass extinctions: Impacts and beyond: Geological Society of America Special Paper 356, p. 395–413, doi:10.1130/0-8137-2356-6.395.

Winguth, A.M.E., and Maier-Reimer, E., 2005, Causes of marine productivity and oxygen changes associated with the Permian-Triassic boundary: A reevaluation with ocean general circulation models: Marine Geology, v. 217, p. 283–304, doi:10.1016/j.margeo.2005.02.011.

Zhang, R., Follows, M.J., Grotzinger, J.P., and Marshall, J., 2001, Could the Late Permian deep ocean have been anoxic?: Paleoceanography, v. 16, p. 317–329, doi:10.1029/2000PA000522.

Manuscript received 12 May 2011
Revised manuscript received 7 September 2011
Manuscript accepted 13 September 2011

Printed in USA

ERRATUM

Simulating Permian–Triassic oceanic anoxia distribution: Implications for species extinction and recovery

Cornelia Winguth and Arne M.E. Winguth

(*Geology*, v.40, p. 127–130, doi:10.1130/G32453.1

A typesetting error occurred during production of this paper, and at all the places where mmol appears in the text or figure captions, it should read μmol instead.